Supplement of Atmos. Chem. Phys., 24, 11207–11226, 2024
https://doi.org/10.5194/acp-24-11207-2024-supplement

Atmospheric Chemistry and Physics
Open Access

Supplement of

Present-day methane shortwave absorption mutes surface warming relative to preindustrial conditions

Robert J. Allen et al.

Correspondence to: Robert J. Allen (rjallen@ucr.edu)

Table S1. Global annual mean total, fast and slow low cloud responses (ΔCLDLOW) for CH_4 and CO_2 perturbations. Responses are shown for shortwave and longwave (SW+LW) radiative effects of CH_4 and CO_2 (e.g., $2.5xCH_{4LW+SW}$); longwave-only radiative effects (LW) of CH_4 and CO_2 (e.g., $2.5xCH_{4LW}$); and shortwave-only radiative effects (SW) of CH_4 and CO_2 (e.g., $2.5xCH_{4SW}$). Total responses come from the coupled ocean atmosphere simulations. Fast responses come from the fixed SST simulations. Slow responses are estimated as the difference (total minus fast). Uncertainty is estimated as 1.65*square root of the pooled variance (i.e., 90% confidence interval). Units are %.

ΔCLDLOW [%]	$2.5xCH_{4LW+SW}$	$2.5xCH_{4LW}$	$2.5xCH_{4SW}$
Total	-0.05 ± 0.16	-0.44 ± 0.09	0.39 ± 0.24
Fast	-0.03 ± 0.08	-0.10 ± 0.07	0.08 ± 0.07
Slow	-0.02 ± 0.18	-0.34 ± 0.11	0.31 ± 0.25

ΔCLDLOW [%]	$5xCH_{4LW+SW}$	$5xCH_{4LW}$	$5xCH_{4SW}$
Total	0.001 ± 0.09	-0.48 ± 0.14	0.48 ± 0.21
Fast	0.02 ± 0.08	-0.20 ± 0.07	0.22 ± 0.10
Slow	-0.02 ± 0.12	-0.28 ± 0.16	0.26 ± 0.24

ΔCLDLOW [%]	$10xCH_{4LW+SW}$	$10xCH_{4LW}$	$10xCH_{4SW}$
Total	-0.11 ± 0.16	-0.89 ± 0.14	0.78 ± 0.23
Fast	-0.01 ± 0.08	-0.37 ± 0.07	0.36 ± 0.10
Slow	-0.10 ± 0.18	-0.52 ± 0.16	0.42 ± 0.26

ΔCLDLOW [%]	$4xCO_{2LW+SW}$	$4xCO_{2LW}$	$4xCO_{2SW}$
Total	-4.05 ± 0.14	-4.43 ± 0.17	0.38 ± 0.23
Fast	-2.04 ± 0.08	-2.13 ± 0.07	0.09 ± 0.09
Slow	-2.01 ± 0.16	-2.30 ± 0.18	0.29 ± 0.21

Table S2. Global mean top-of-the-atmosphere energy decomposition for CH_4 and CO_2 perturbations based on the equation ΔN=ΔF+αΔTAS, where ΔN is the change in the global mean TOA net energy flux [W m^{-2}]; ΔTAS is the change in global mean near-surface air temperature [K]; ΔF is the change in the global mean TOA net energy flux [W m^{-2}] when ΔTAS = 0 (i.e., the effective radiative forcing, ERF); and α is the net feedback parameter [W m^{-2} K^{-1}]. Here, ΔN and ΔTAS are calculated using 40 years (years 51-90) from the coupled ocean-atmosphere simulations. ΔF is approximated using 30 years (years 3-32) from atmosphere-only simulations which feature climatologically fixed SST and sea-ice distributions (fSST). Uncertainty is estimated as 1.65*square root of the pooled variance. The net feedback parameter α is calculated from the slope of the regression line that connects two points: (ΔTAS, ΔN) from the coupled simulations and (ΔTAS, ΔN) from the fSST simulations. Using the surface-temperature adjusted ΔN from fSST simulations yields similar results. Uncertainty in α is estimated as the 1-sigma uncertainty estimate of the slope (the regression accounts for uncertainty in both ΔTAS and ΔN). Corresponding values for the climate sensitivity parameter (λ; K [W m^{-2}]$^{-1}$) are also included, obtained by regressing (ΔN, ΔTAS) from the coupled simulations and (ΔN, ΔTAS) from the fSST simulations. Also included is an alternate estimate of the climate feedback parameter [α_k; W m^{-2} K^{-1}] as estimated by normalizing the slow response's radiative flux decomposition (based on the radiative kernel method) by its corresponding change in global mean near-surface air temperature.

	2.5xCH_{4LW+SW}	**2.5xCH_{4LW}**	**2.5xCH_{4SW}**
ΔN	0.04 ± 0.20	0.21 ± 0.20	-0.17 ± 0.31
ΔF	0.43 ± 0.12	0.53 ± 0.10	-0.10 ± 0.13
ΔTAS	0.25 ± 0.05	0.36 ± 0.05	-0.10 ± 0.07
α	-1.70 ± 1.39	-1.00 ± 0.86	0.87 ± 3.41
α_k	-1.59 ± 0.88	-0.85 ± 0.63	1.03 ± 3.29
λ	0.59 ± 0.48	1.00 ± 0.86	-1.14 ± 4.46

	5xCH_{4LW+SW}	**5xCH_{4LW}**	**5xCH_{4SW}**
ΔN	0.11 ± 0.20	0.24 ± 0.20	-0.13 ± 0.28
ΔF	0.98 ± 0.12	1.20 ± 0.10	-0.22 ± 0.17
ΔTAS	0.45 ± 0.05	0.68 ± 0.05	-0.23 ± 0.07
α	-2.21 ± 0.88	-1.56 ± 0.49	-0.40 ± 1.60
α_k	-2.14 ± 0.53	-1.52 ± 0.29	-0.40 ± 1.30
λ	0.45 ± 0.18	0.64 ± 0.20	2.48 ± 9.81

	10xCH_{4LW+SW}	**10xCH_{4LW}**	**10xCH_{4SW}**
ΔN	0.33 ± 0.20	0.50 ± 0.20	-0.17 ± 0.31
ΔF	1.70 ± 0.13	2.14 ± 0.08	-0.44 ± 0.15
ΔTAS	0.85 ± 0.05	1.24 ± 0.05	-0.39 ± 0.07
α	-1.80 ± 0.44	-1.45 ± 0.26	-0.73 ± 1.08
α_k	-1.81 ± 0.28	-1.45 ± 0.17	-0.72 ± 0.86
λ	0.55 ± 0.13	0.69 ± 0.12	1.37 ± 2.02

	$4xCO_{2LW+SW}$	**$4xCO_{2LW}$**	**$4xCO_{2SW}$**
ΔN	2.82 ± 0.17	3.06 ± 0.20	-0.24 ± 0.26
ΔF	8.46 ± 0.12	8.82 ± 0.12	-0.35 ± 0.15
ΔTAS	5.45 ± 0.07	5.84 ± 0.08	-0.38 ± 0.12
α	-1.18 ± 0.06	-1.11 ± 0.06	-0.31 ± 0.93
α_k	-1.33 ± 0.05	-1.30 ± 0.06	-0.91 ± 0.68
λ	0.85 ± 0.04	0.90 ± 0.05	3.27 ± 9.98

Table S3. Global mean precipitation decomposition for CH_4 and CO_2 perturbations based on the equation $L_c\Delta P = A + \eta\Delta TAS$, where L_c is the latent heat of condensation of water vapor with a value of 29 W m^{-2} (mm $day^{-1})^{-1}$; ΔP is the change in the global mean precipitation [mm day^{-1}]; ΔTAS is the change in global mean near-surface air temperature [K]; A is an adjustment term that accounts for the change in precipitation independent of any change in surface temperature [W m^{-2}], which can be further decomposed into SWC+LWC+SH, where SWC is the net shortwave radiative cooling of the atmosphere; LWC is the net longwave radiative cooling of the atmosphere; and SH is the downwards sensible heat flux at the surface (positive values for these three terms indicate cooling and energy loss). The hydrological sensitivity parameter is η [W m^{-2} K^{-1}]. Here, ΔP and ΔTAS are calculated using 50 years (years 51-90) from the coupled ocean-atmosphere simulations. A is approximated using 30 years (years 3-32) from atmosphere-only simulations which feature climatologically fixed SST and sea-ice distributions (fSST). Uncertainty is estimated as 1.65*square root of the pooled variance. The hydrological sensitivity parameter η is calculated from the slope on the ordinary least squares regression line that connects two points: (ΔTAS, ΔP) from the coupled simulations and (ΔTAS, ΔP) from the fSST simulations. Uncertainty in η is estimated as the 1-sigma uncertainty estimate of the slope (the regression accounts for uncertainty in both ΔTAS and ΔP).

	2.5xCH_{4LW+SW}	**2.5xCH_{4LW}**	**2.5xCH_{4SW}**
$L_c\Delta P$	0.119 ± 0.18	0.355 ± 0.18	-0.235 ± 0.28
A	-0.303 ± 0.09	-0.215 ± 0.07	-0.088 ± 0.09
SWC	-0.204 ± 0.03	-0.030 ± 0.02	-0.174 ± 0.03
LWC	-0.151 ± 0.09	-0.245 ± 0.07	0.094 ± 0.10
SH	0.051 ± 0.03	0.061 ± 0.02	-0.009 ± 0.03
ΔTAS	0.25 ± 0.05	0.36 ± 0.05	-0.10 ± 0.07
η	1.83 ± 0.87	1.78 ± 0.60	1.84 ± 3.68

	5xCH_{4LW+SW}	**5xCH_{4LW}**	**5xCH_{4SW}**
$L_c\Delta P$	0.423 ± 0.17	1.023 ± 0.16	-0.60 ± 0.22
A	-0.649 ± 0.08	-0.509 ± 0.08	-0.140 ± 0.12
SWC	-0.492 ± 0.03	-0.048 ± 0.03	-0.445 ± 0.04
LWC	-0.275 ± 0.09	-0.566 ± 0.08	0.291 ± 0.12
SH	0.121 ± 0.03	0.103 ± 0.02	0.018 ± 0.03
ΔTAS	0.45 ± 0.05	0.68 ± 0.05	-0.23 ± 0.07
η	2.73 ± 0.48	2.49 ± 0.29	2.06 ± 1.12

	10xCH_{4LW+SW}	**10xCH_{4LW}**	**10xCH_{4SW}**
$L_c\Delta P$	0.72 ± 0.16	1.84 ± 0.17	-1.12 ± 0.25
A	-1.16 ± 0.08	-0.866 ± 0.07	-0.290 ± 0.10
SWC	-0.917 ± 0.03	-0.066 ± 0.02	-0.850 ± 0.04
LWC	-0.459 ± 0.09	-0.978 ± 0.07	0.519 ± 0.11
SH	0.220 ± 0.03	0.181 ± 0.03	0.039 ± 0.04
ΔTAS	0.85 ± 0.05	1.24 ± 0.05	-0.39 ± 0.07
η	2.47 ± 0.24	2.39 ± 0.16	2.24 ± 0.73

	$4xCO_{2LW+SW}$	$4xCO_{2LW}$	$4xCO_{2SW}$
$L_c\Delta P$	6.96 ± 0.19	7.87 ± 0.20	-0.913 ± 0.30
A	-4.91 ± 0.09	-4.84 ± 0.07	-0.077 ± 0.11
SWC	-0.579 ± 0.03	-0.173 ± 0.03	-0.406 ± 0.04
LWC	-3.99 ± 0.09	-4.34 ± 0.08	0.350 ± 0.12
SH	-0.368 ± 0.03	-0.353 ± 0.02	-0.016 ± 0.03
ΔTAS	5.45 ± 0.07	5.84 ± 0.08	-0.38 ± 0.12
η	2.47 ± 0.04	2.46 ± 0.04	2.31 ± 0.89

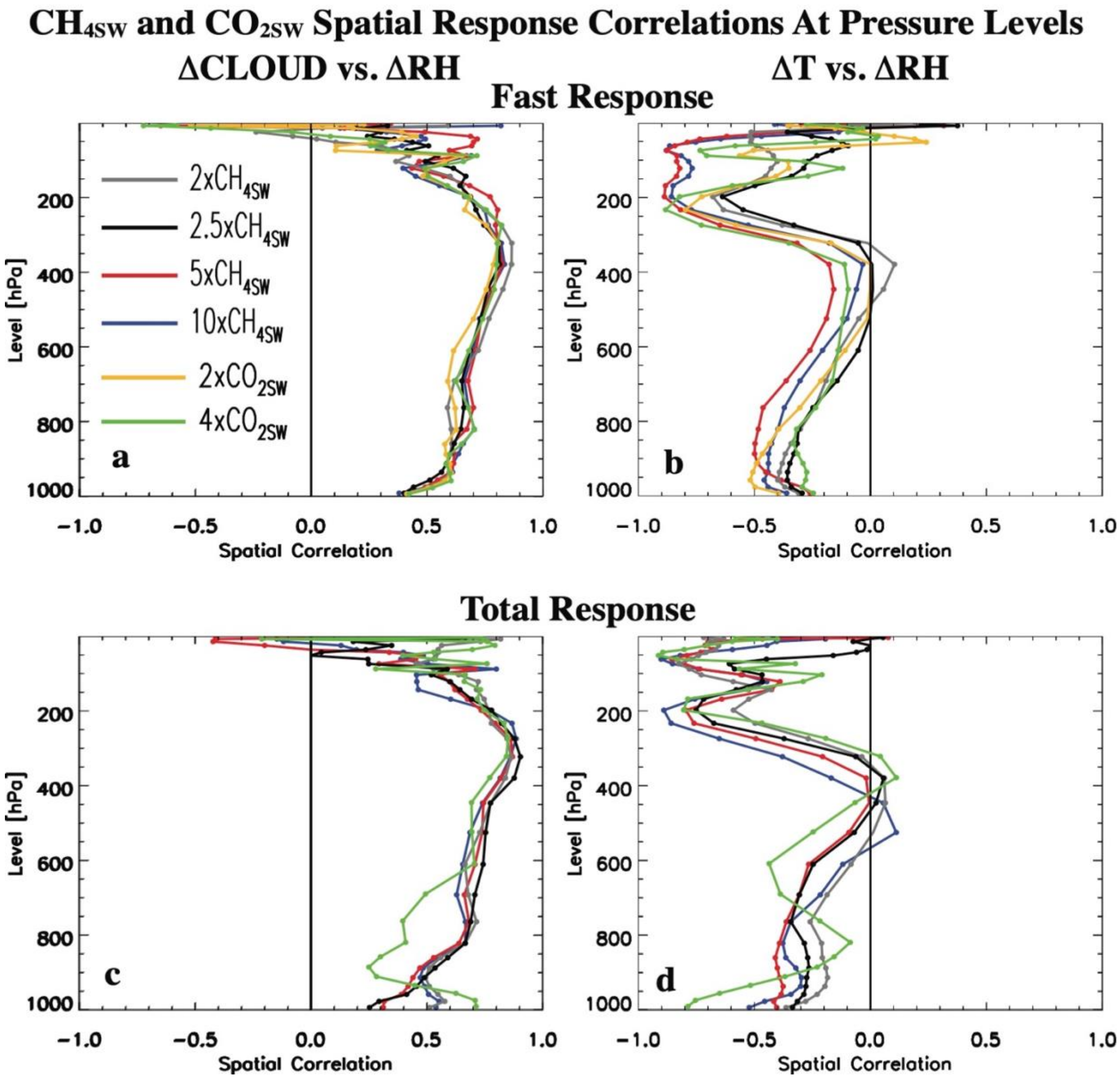

Figure S1. CH_{4SW} and CO_{2SW} spatial response correlations at each pressure level. Annual mean spatial correlations at each pressure level for (a, c) ΔCLOUD versus ΔRH; and (b, d) ΔT versus ΔRH for (a-b) the fast response and (c-d) the total response for 2xCH_{4SW} (gray); 2.5xCH_{4SW} (black); 5xCH_{4SW} (red); 10xCH_{4SW} (blue); 2xCO_{2SW} (gold); and 4xCO_{2SW} (green). A significant correlation at the 90% confidence level, based on a standard t-test, is denoted by solid dots. Climatologically fixed SST simulations are used to estimate the fast responses. Total climate responses are estimated using data from coupled ocean-atmosphere CESM2 simulations. 2xCO_2 coupled simulations were not performed (i.e., no gold line in panels c-d).

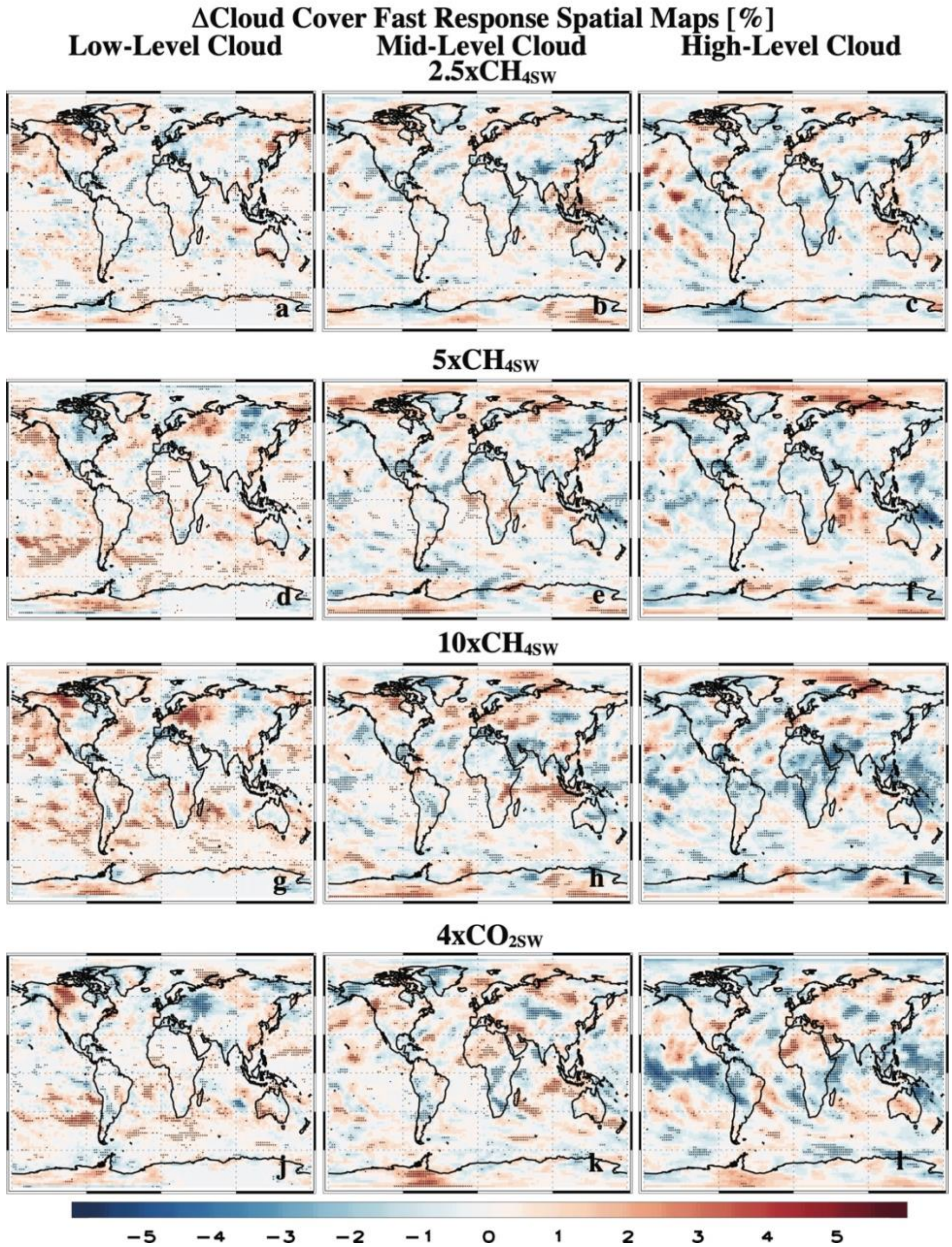

Figure S2. Spatial cloud cover fast responses under CH_{4SW} and CO_{2SW}. Annual mean spatial distribution of the fast responses of (a, d, g, j) low-cloud cover; (b, e, h, k) mid-level cloud cover; and (c, f, i, l) high-level cloud cover under (a-c) 2.5xCH_{4SW}; (d-f) 5xCH_{4SW}; (g-i) 10xCH_{4SW}; and (j-l) 4xCO_{2SW}. A significant response at the 90% confidence level, based on a standard t-test, is denoted by solid dots. Fast responses are estimated from the fixed climatological sea surface temperature simulations. Units are %.

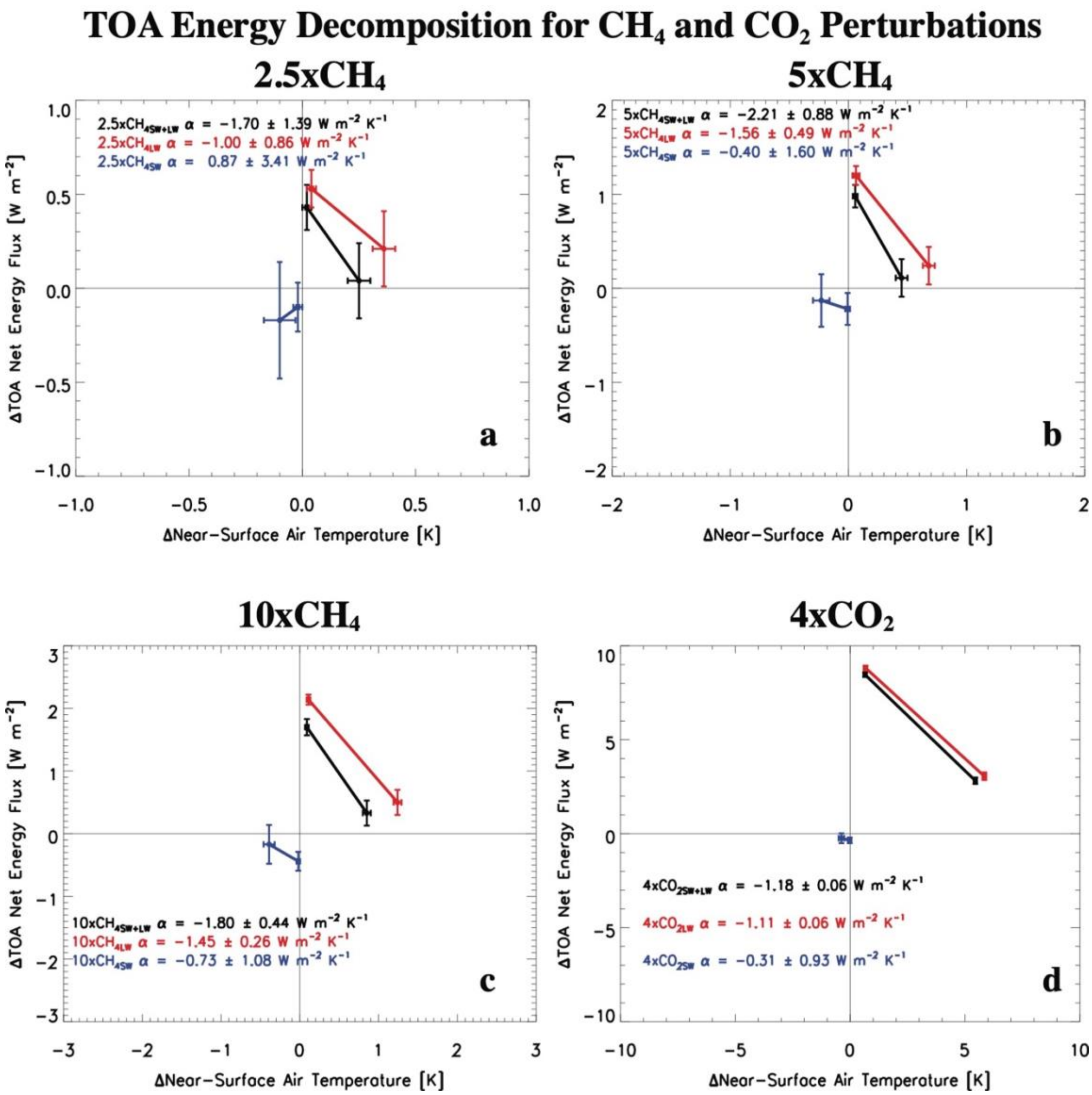

Figure S3. Global mean TOA energy decomposition for CH_4 and CO_2 perturbations based on the equation $\Delta N = \Delta F + \alpha \Delta TAS$. ΔN is the change in the global mean TOA net energy flux [W m^{-2}]; ΔTAS is the change in global mean near-surface air temperature [K]; and ΔF is the change in the global mean TOA net energy flux [W m^{-2}] when $\Delta TAS = 0$ (i.e., the effective radiative forcing, ERF). Uncertainty is estimated as 1.65*square root of the pooled variance. α is the net feedback parameter [W m^{-2} K^{-1}] and is calculated from the slope of the ordinary least squares regression line that connects two points: (ΔTAS, ΔN) from the coupled simulations and (ΔTAS, ΔN) from the fSST simulations. Uncertainty in α is estimated as the 1-sigma uncertainty estimate of the slope (the regression accounts for uncertainty in both ΔTAS and ΔN).

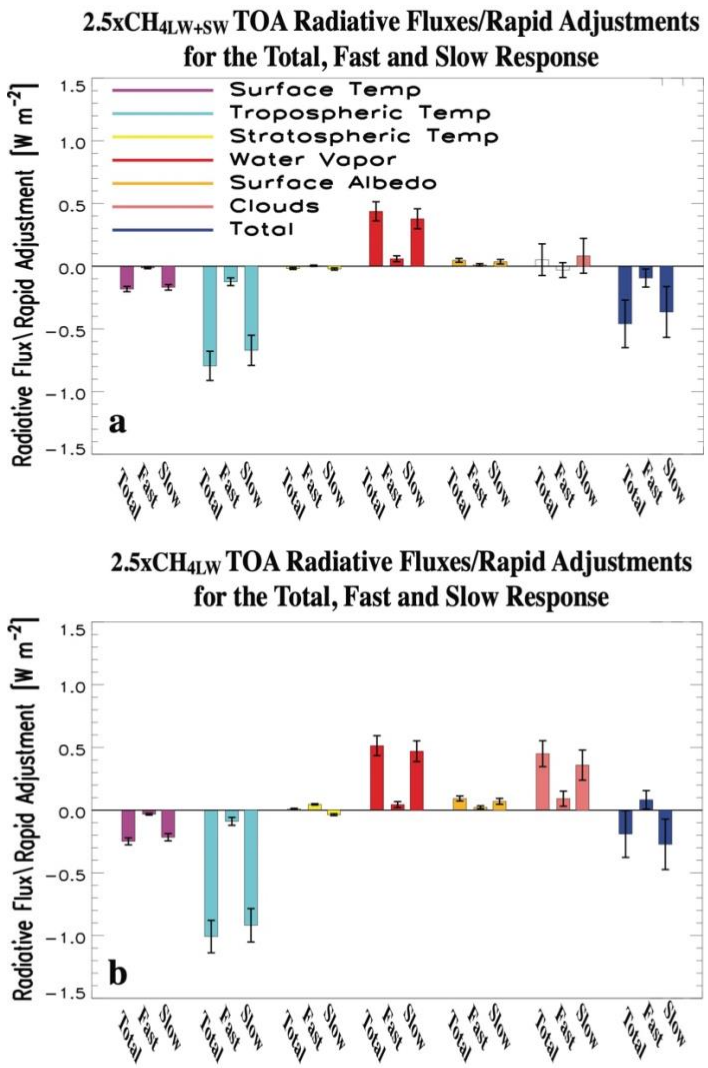

Figure S4. 2.5xCH_{4LW+SW} and 2.5xCH_{4LW} top-of-the-atmosphere radiative flux decomposition for the total response, fast response (rapid adjustment) and slow response. Global annual mean top-of-the-atmosphere (TOA) surface temperature (purple), tropospheric temperature (cyan), stratospheric temperature (yellow), water vapor (red), surface albedo (orange), cloud (pink) and total (blue) radiative flux decomposition for (a) 2.5xCH_{4LW+SW} and (b) 2.5xCH_{4LW}. The total response (from the coupled ocean atmosphere simulations) is represented by the first bar in each like-colored set of three bars; the rapid adjustment (fast response from fixed climatological sea surface temperature simulations) is represented by the second bar; and the surface-temperature-induced response (slow response; estimated as the difference of the total response minus the fast response) is represented by the third bar. Uncertainty is quantified using the 90% confidence interval; unfilled bars denote responses that are not significant at the 90% confidence level. Units are W m^{-2}.

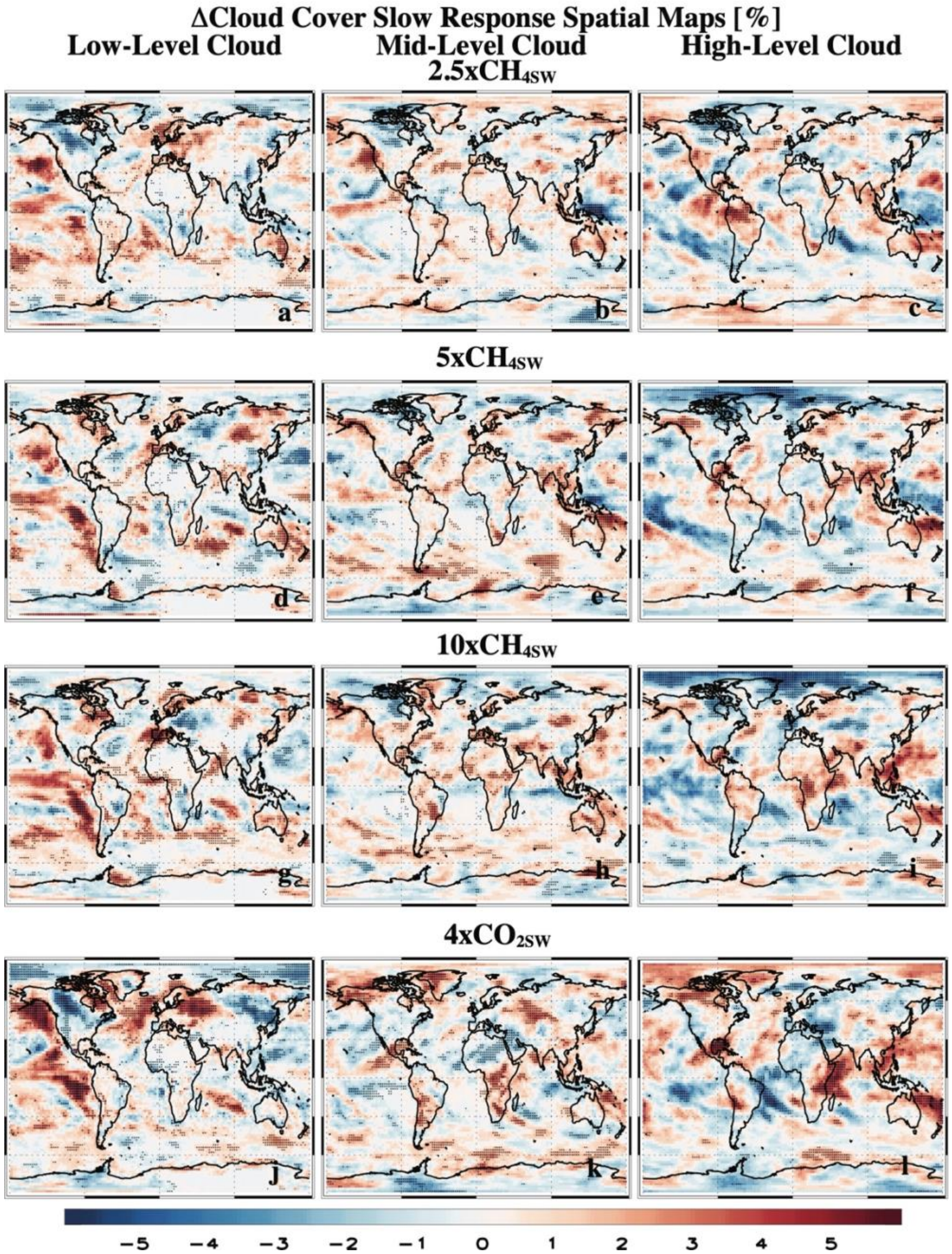

Figure S5. Spatial cloud cover slow responses under CH_{4SW} and CO_{2SW}. Annual mean spatial distribution of the slow responses of (a, d, g, j) low-cloud cover; (b, e, h, k) mid-level cloud cover; and (c, f, i, l) high-level cloud cover under (a-c) 2.5xCH_{4SW}; (d-f) 5xCH_{4SW}; (g-i) 10xCH_{4SW}; and (j-l) 4xCO_{2SW}. A significant response at the 90% confidence level, based on a standard t-test, is denoted by solid dots. Slow responses are estimated as the difference of the total response minus the fast response. Units are %.

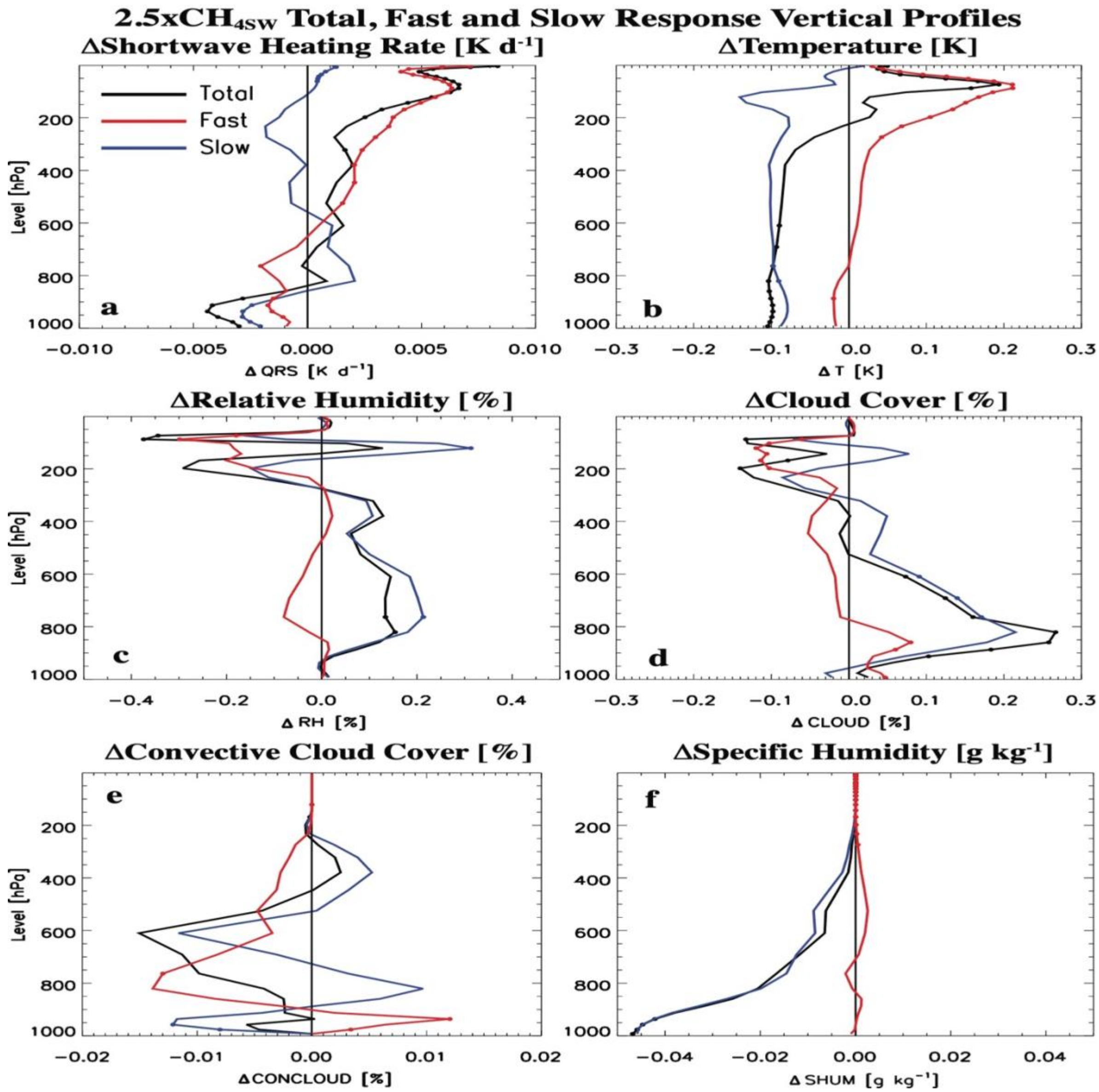

Figure S6. 2.5xCH_{4SW} total, fast and slow vertical profile responses. 2.5xCH_{4SW} annual mean global mean vertical response profiles of (a) shortwave heating rate (QRS; units are K d^{-1}); (b) air temperature (T; units are K); and (c) relative humidity (RH; units are %); (d) cloud cover (CLOUD; units are %); (e) convective cloud cover (CONCLOUD; units are %); and (f) specific humidity (SHUM; units are g kg^{-1}) for the total (black); fast (red) and slow (blue) response. A significant response at the 90% confidence level, based on a standard t-test, is denoted by solid dots. Climatologically fixed SST simulations are used to estimate the fast responses. Total climate responses are estimated using data from coupled ocean-atmosphere CESM2 simulations. The slow response is estimated as the difference of the total response minus the fast response.

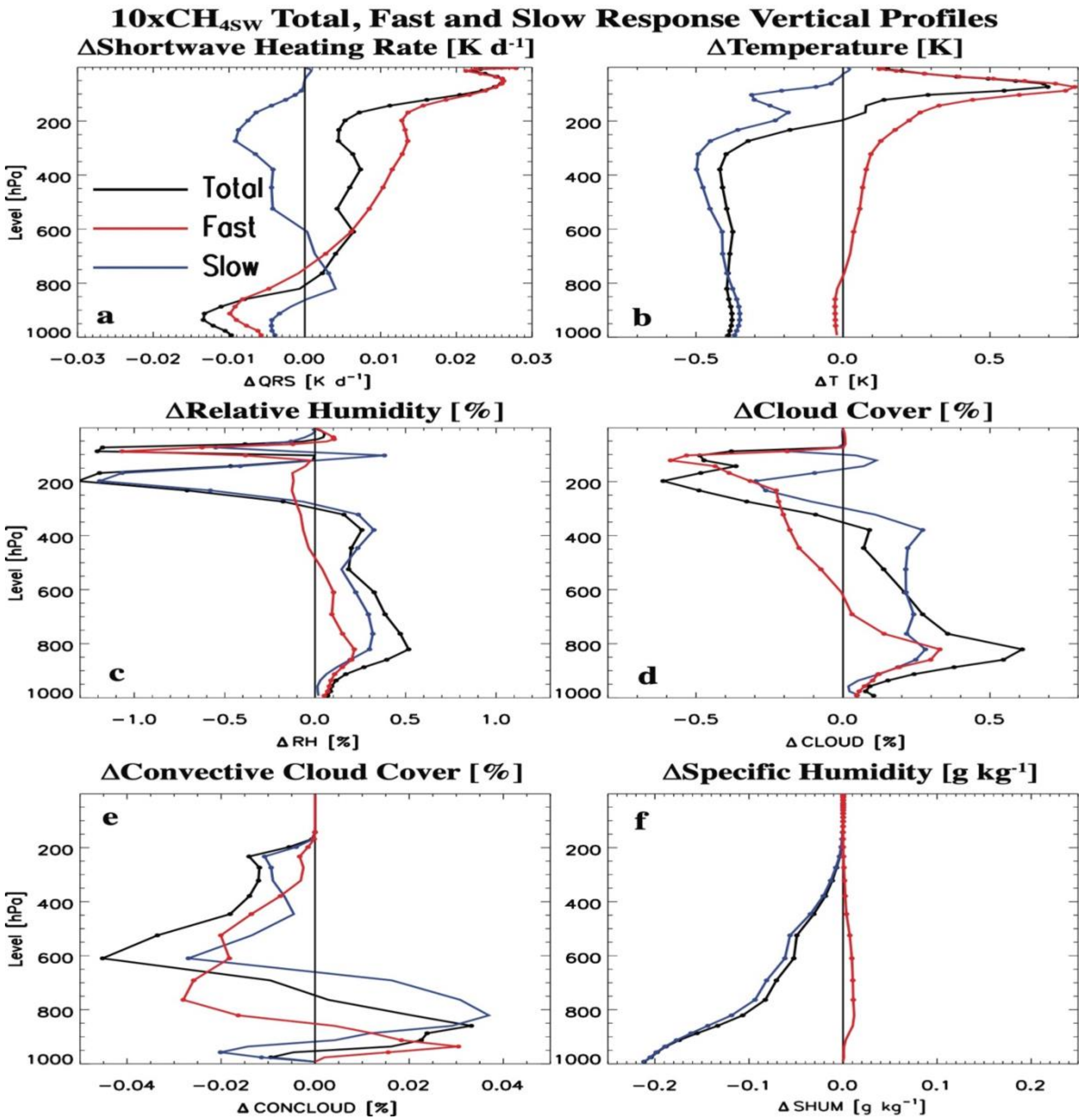

Figure S7. 10xCH_{4SW} total, fast and slow vertical profile responses. 10xCH_{4SW} annual mean global mean vertical response profiles of (a) shortwave heating rate (QRS; units are K d^{-1}); (b) air temperature (T; units are K); and (c) relative humidity (RH; units are %); (d) cloud cover (CLOUD; units are %); (e) convective cloud cover (CONCLOUD; units are %); and (f) specific humidity (SHUM; units are g kg^{-1}) for the total (black); fast (red) and slow (blue) response. A significant response at the 90% confidence level, based on a standard t-test, is denoted by solid dots. Climatologically fixed SST simulations are used to estimate the fast responses. Total climate responses are estimated using data from coupled ocean-atmosphere CESM2 simulations. The slow response is estimated as the difference of the total response minus the fast response.

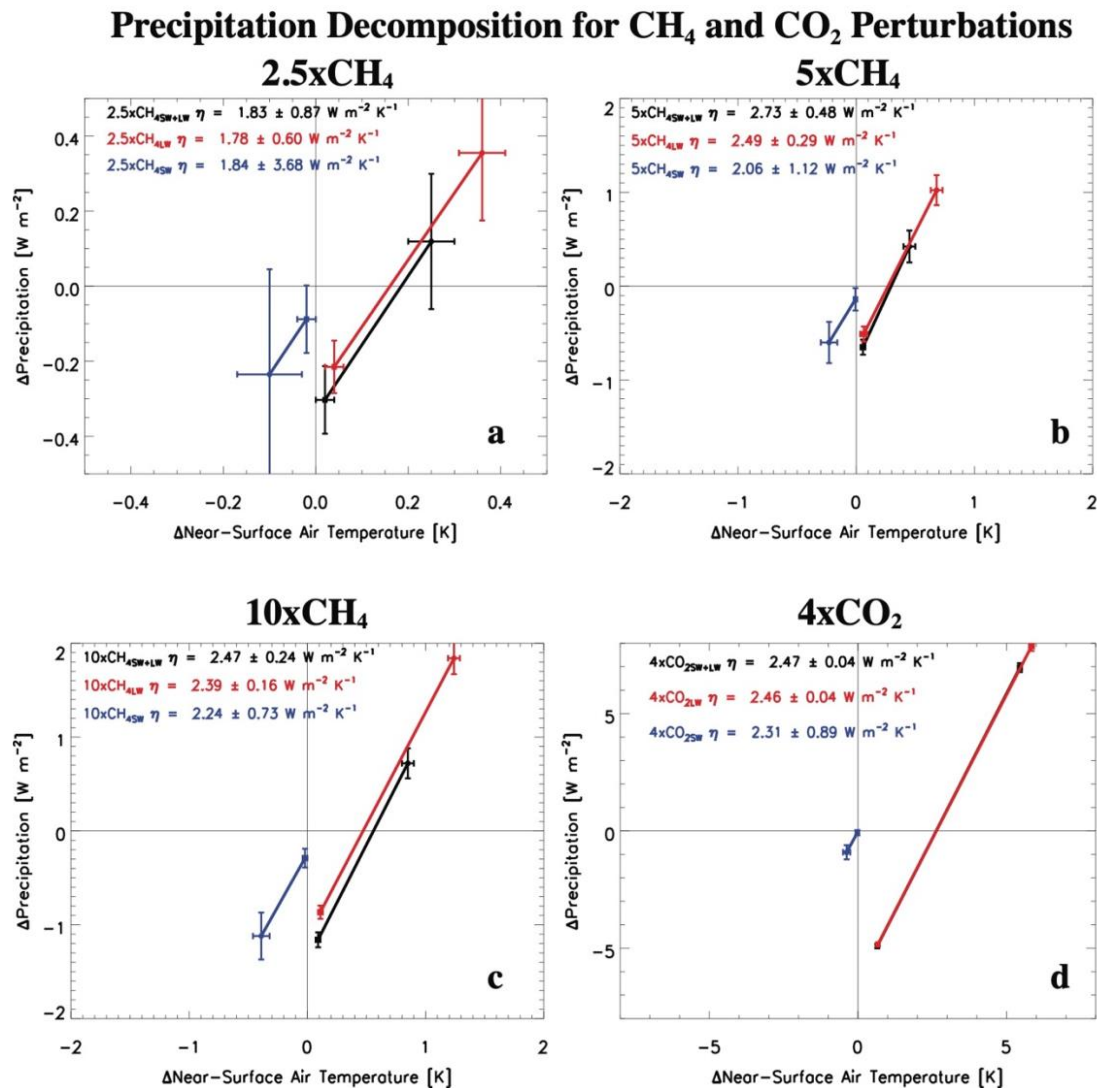

Figure S8. Global mean precipitation decomposition for CH_4 and CO_2 perturbations based on the equation $L_c\Delta P = A + \eta\Delta TAS$. L_c is the latent heat of condensation of water vapor with a value of 29 W m^{-2} (mm $day^{-1})^{-1}$; ΔP is the change in the global mean precipitation [mm day^{-1}]; ΔTAS is the change in global mean near-surface air temperature [K]; A is an adjustment term that accounts for the change in precipitation independent of any change in surface temperature [W m^{-2}]. Uncertainty is estimated as 1.65* square root of the pooled variance. η is the hydrological sensitivity parameter [W m^{-2} K^{-1}] and is calculated from the slope of the ordinary least squares regression line that connects two points: (ΔTAS, ΔP) from the coupled simulations and (ΔTAS, ΔP) from the fSST simulations. Uncertainty in η is estimated as the 1-sigma uncertainty estimate of the slope (the regression accounts for uncertainty in both ΔTAS and ΔP).

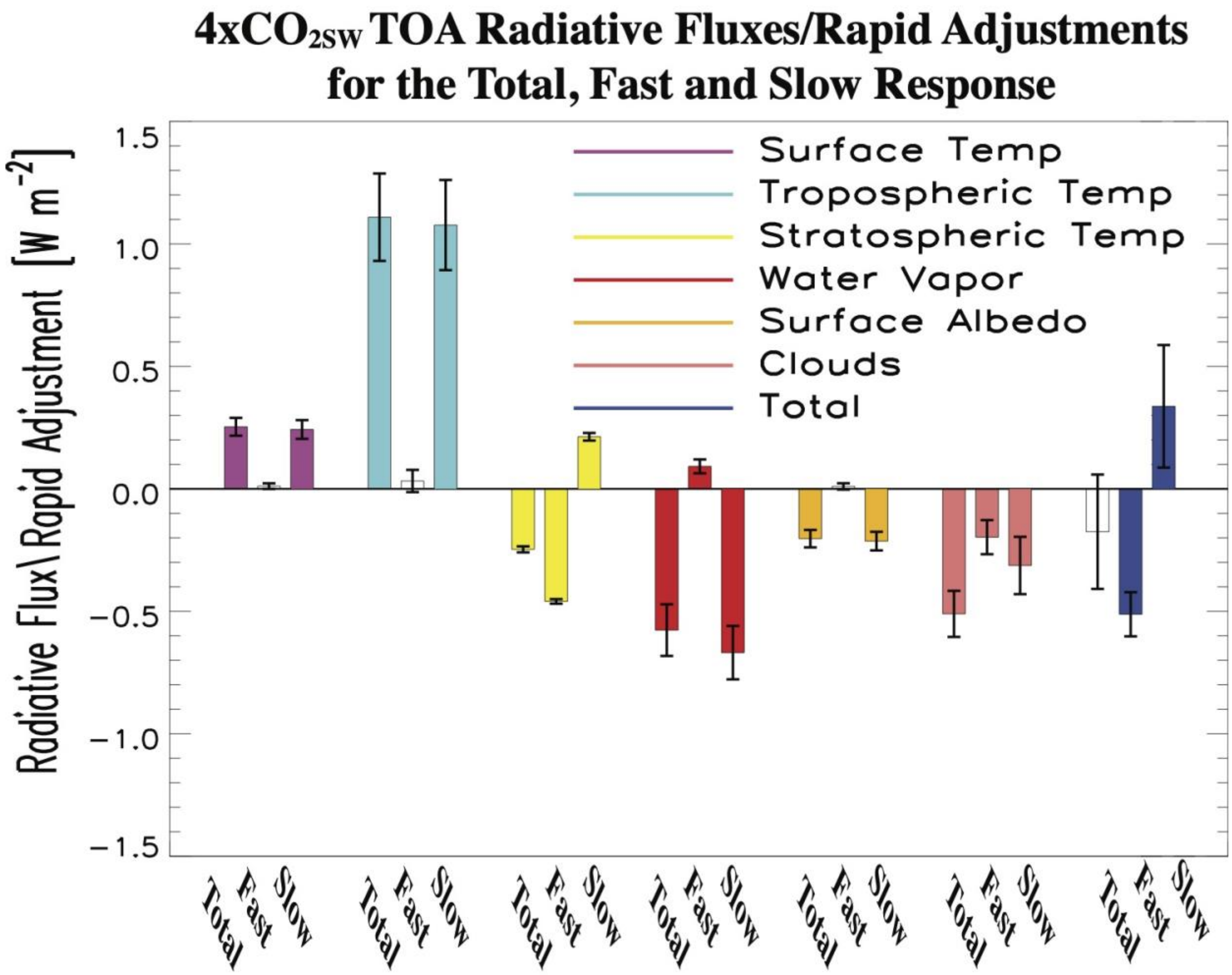

Figure S9. $4xCO_{2SW}$ top-of-the-atmosphere radiative flux decomposition for the total response, fast response (rapid adjustment) and slow response. Global annual mean top-of-the-atmosphere (TOA) surface temperature (purple), tropospheric temperature (cyan), stratospheric temperature (yellow), water vapor (red), surface albedo (orange), cloud (pink) and total (blue) radiative flux decomposition for $4xCO_{2SW}$. The total response (from the coupled ocean atmosphere simulations) is represented by the first bar in each like-colored set of three bars; the rapid adjustment (fast response from fixed climatological sea surface temperature simulations) is represented by the second bar; and the surface-temperature-induced response (slow response; estimated as the difference of the total response minus the fast response) is represented by the third bar. Uncertainty is quantified using the 90% confidence interval; unfilled bars denote responses that are not significant at the 90% confidence level. Units are W m^{-2}.

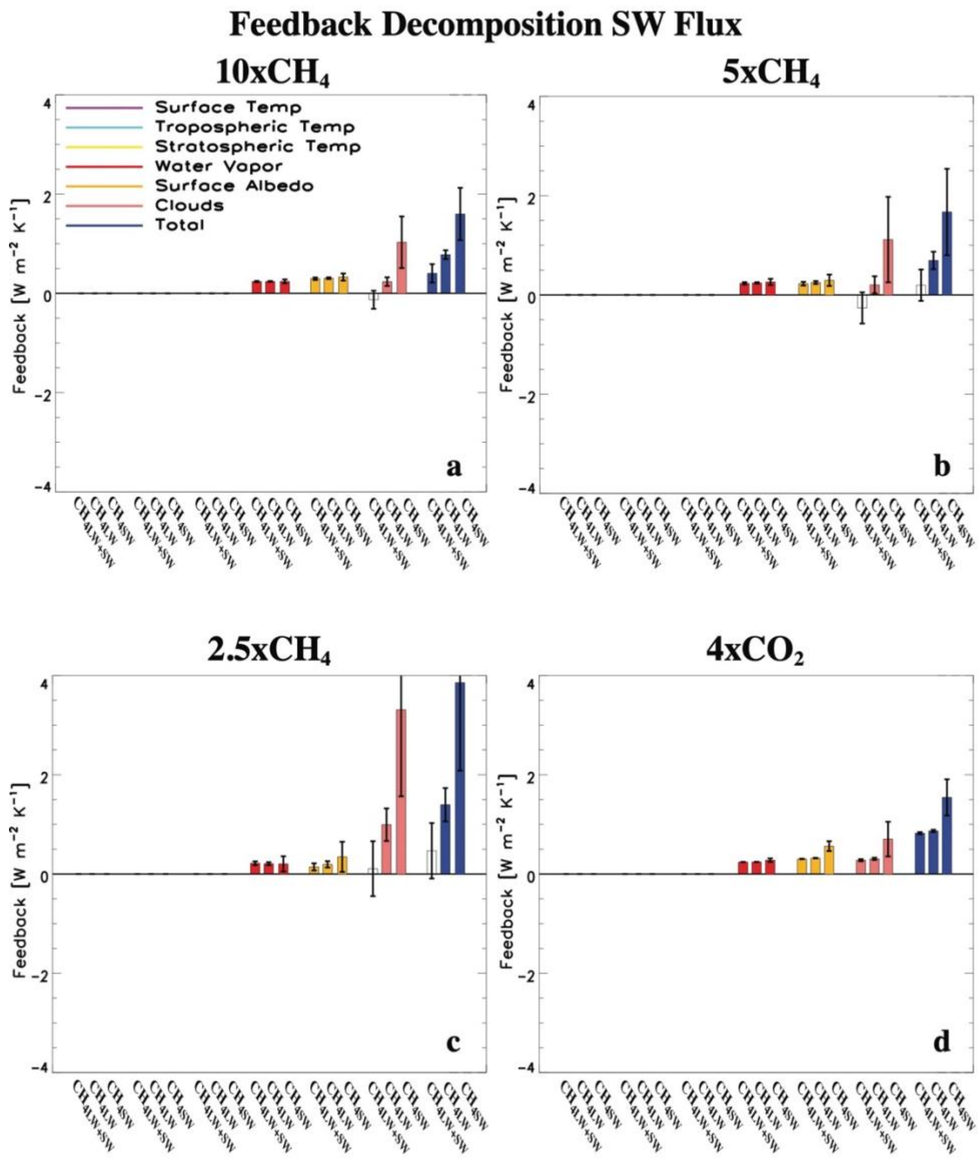

Figure S10. Feedback decomposition for SW flux based on the radiative kernel method. Global annual mean top-of-the-atmosphere (TOA) surface temperature (purple), tropospheric temperature (cyan), stratospheric temperature (yellow), water vapor (red), surface albedo (orange), cloud (pink) and total (blue) feedback decomposition for SW radiation, as estimated by normalizing the slow response's radiative flux decomposition by the corresponding change in global mean near-surface air temperature. Feedbacks are decomposed into CH_4 and CO_2 longwave and shortwave radiative effects (e.g., CH_{4LW+SW}; first bar in each like-colored set of three bars), longwave radiative effects (e.g., CH_{4LW}; second bar) and shortwave radiative effects (e.g., CH_{4SW}; third bar). Uncertainty is quantified using the 90% confidence interval; unfilled bars denote responses that are not significant at the 90% confidence level. Units are W m^{-2} K^{-1}.

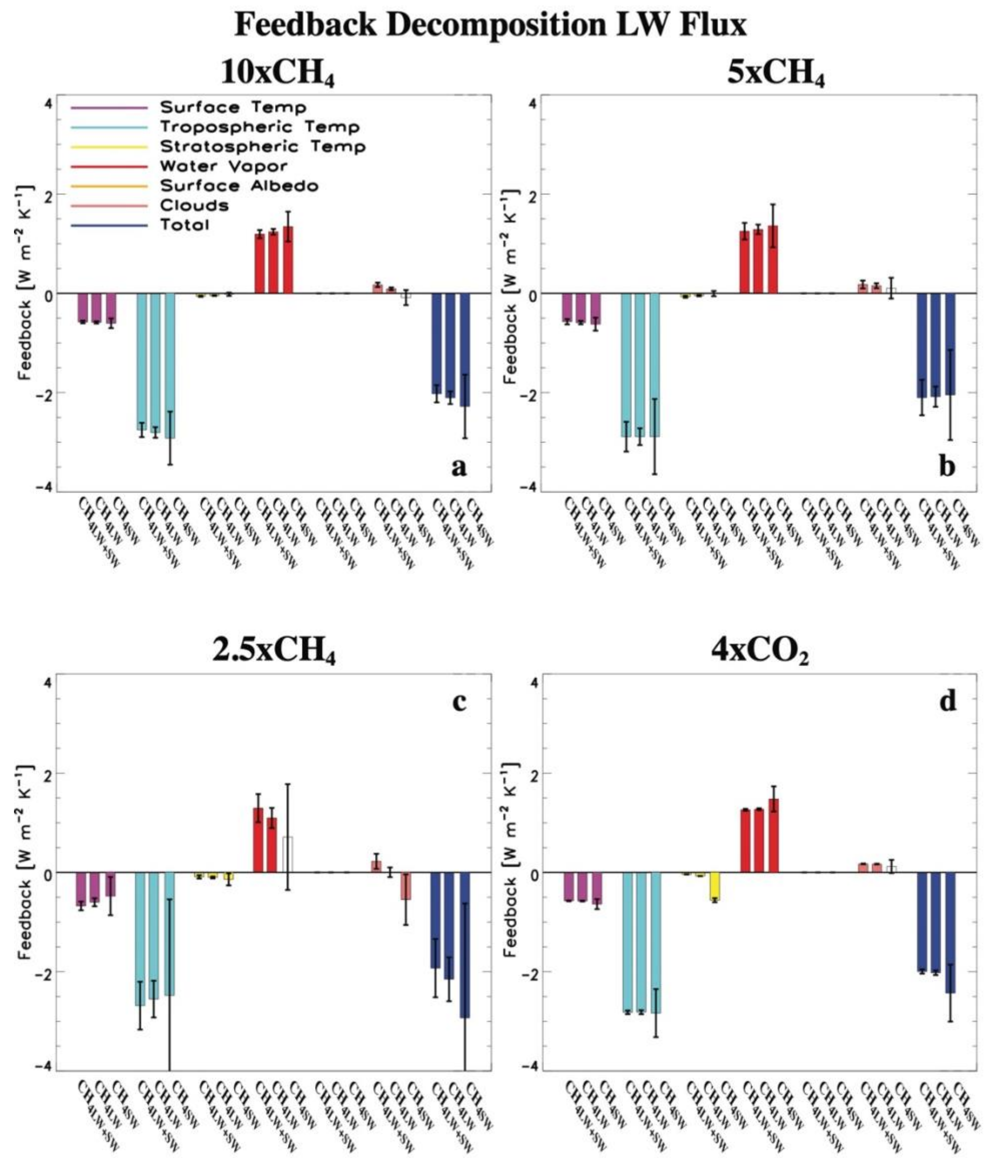

Figure S11. Feedback decomposition for LW flux based on the radiative kernel method. Global annual mean top-of-the-atmosphere (TOA) surface temperature (purple), tropospheric temperature (cyan), stratospheric temperature (yellow), water vapor (red), surface albedo (orange), cloud (pink) and total (blue) feedback decomposition for LW radiation, as estimated by normalizing the slow response's radiative flux decomposition by the corresponding change in global mean near-surface air temperature. Feedbacks are decomposed into CH_4 and CO_2 longwave and shortwave radiative effects (e.g., CH_{4LW+SW}; first bar in each like-colored set of three bars), longwave radiative effects (e.g., CH_{4LW}; second bar) and shortwave radiative effects (e.g., CH_{4SW}; third bar). Uncertainty is quantified using the 90% confidence interval; unfilled bars denote responses that are not significant at the 90% confidence level. Units are W m^{-2} K^{-1}.